

Copper(II) Complexes with New Polyodal Ligands Presenting Axial–Equatorial Phenoxo Bridges {2-[(Bis(2-pyridylmethyl)-amino)methyl]-4-methylphenol, 2-[(Bis(2-pyridylmethyl)-amino)methyl]-4-methyl-6-(methylthio)phenol}: Examples of Ferromagnetically Coupled Bi- and Trinuclear Copper(II) Complexes

Jorge Manzur* and Hector Mora

Departamento de Ciencia de los Materiales, Facultad de Ciencias Físicas y Matemáticas, Universidad de Chile, Tupper 2069, Santiago, Chile

Andrés Vega

Departamento de Ciencias Químicas, Facultad de Ecología y Recursos Naturales, Universidad Nacional Andrés Bello, República 275, Santiago, Chile

Evgenia Spodine and Diego Venegas-Yazigi

Departamento de Química Inorgánica y Analítica, Facultad de Ciencias Químicas y Farmacéuticas, CIMAT, Universidad de Chile, Olivos 1007, Santiago, Chile

María Teresa Garland

Departamento de Física, Facultad de Ciencias Físicas y Matemáticas, CIMAT, Universidad de Chile, Tupper 2069, Santiago, Chile

M. Salah El Fallah and Albert Escuer

Departament de Química Inorgánica, Universitat de Barcelona, Martí i Franqués 1-11, 08028-Barcelona, Spain

Received March 21, 2007

Two new ligands, 2-[(bis(2-pyridylmethyl)amino)methyl]-4-methylphenol (HL) and 2-[(bis(2-pyridylmethyl)amino)methyl]-4-methyl-6-(methylthio)phenol (HSL), were synthesized and were used to prepare the trinuclear copper(II) complex $\{[\text{CuSL}(\text{Cl})]_2\text{Cu}\}(\text{PF}_6)_2 \cdot \text{H}_2\text{O}$ (**1**) and the corresponding binuclear complexes $[\text{Cu}_2(\text{SL})_2](\text{PF}_6)_2$ (**2**) and $[\text{Cu}_2\text{L}_2](\text{PF}_6)_2$ (**3**). The crystal structure of **1** shows two different coordination environments: two square base pyramidal centers (Cu1 and Cu1a, related by a C_2 axes), acting as ligands of a distorted square planar copper center (Cu2) by means of the sulfur atom of the SCH_3 substituent and the bridging phenoxo oxygen atom of the ligand ($\text{Cu2-S} = 2.294 \text{ \AA}$). Compounds **2** and **3** show two equivalent distorted square base pyramidal copper(II) centers, bridged in an axial–equatorial fashion by two phenoxo groups, thus defining an asymmetric Cu_2O_2 core. A long copper–sulfur distance measured in **2** ($2.9261(18) \text{ \AA}$) suggests a weak bonding interaction. This interaction induces a torsion angle between the methylthio group and the phenoxo plane resulting in a dihedral angle of $41.4(5)^\circ$. A still larger distortion is observed in **1** with a dihedral angle of $74.0(6)^\circ$. DFT calculations for **1** gave a ferromagnetic exchange between first neighbors interaction, the calculated J value for this interaction being $+11.7 \text{ cm}^{-1}$. In addition, an antiferromagnetic exchange for **1** was obtained for the second neighbor interaction with a J value of -0.05 cm^{-1} . The Bleaney–Bowers equation was used to fit the experimental magnetic susceptibility data for **2** and **3**; the best fit was obtained with J values of $+3.4$ and -16.7 cm^{-1} , respectively. DFT calculations for **2** and **3** confirm the nature and the values of the J constants obtained by the fit of the experimental data. ESR and magnetic studies on the reported compounds show a weak exchange interaction between the copper(II) centers. The low values obtained for the coupling constants can be explained in terms of a poor overlap between the magnetic orbitals, due to the axial–equatorial phenoxo bridging mode observed in these complexes.

Introduction

Copper chemistry from a magneto–structural point of view is a very extensively studied area, both experimentally and

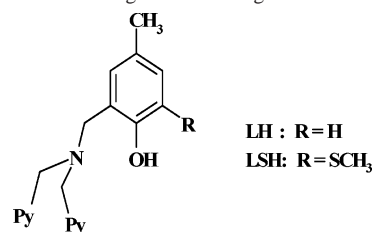
theoretically, especially with respect to binuclear systems. However, reports on trinuclear and higher nuclearity copper compounds are rather scarce. For trinuclear species the reported data show that the triangular arrangement is more common than the linear geometry.¹

* To whom correspondence should be addressed. E-mail: jmanzur@dq.uchile.cl.

Different parameters have been shown to influence the magnetic behavior of these coordination compounds. Binuclear copper(II) complexes bridged by hydroxide² or alkoxide^{3,4} groups have been studied from a magneto-structural point of view, and linear correlations have been found between the Cu–O–Cu bridging angle (θ) and the coupling constant (J) for these compounds. A similar linear correlation between the Cu–O–Cu bridging angle (θ) and the coupling constant (J) has been proposed by Thompson et al.⁵ for the binuclear macrocyclic complexes bridged by a pair of phenoxide groups. For the studied complexes both phenoxo bridges coordinate the metal atoms in an equatorial–equatorial fashion and show strong antiferromagnetic exchange. However, deviation from this ideal configuration results in a large difference from the predicted value for J .⁶ Since the extent of the coupling interaction is strongly structure dependent in single-phenoxo-bridged binuclear copper(II) complexes, magnetic interactions ranging from ferromagnetic to antiferromagnetic have been reported,^{6–9} the ferromagnetic interaction in polynuclear copper(II) complexes being comparatively rare.¹

Several types of ligand systems that can bind two metal ions in close proximity have been studied due to their interesting catalytic properties and the possibilities for magnetic interaction between two metal ions.^{10–12} These studies offer complementary information about the magnetic exchange mechanism between metal centers, which is useful in finding suitable building blocks for the assembly of new magnetic materials¹³ and in the development of new redox catalysts for reactions other than biologically important ones. Pyridylaminophenols can act as polydentate ligands, producing different polymetallic species, depending on the synthetic conditions. We herein report the synthesis and magneto-structural characterization of three coordination compounds: [Cu₃(SL)₂(Cl)₂](PF₆)₂ (**1**), [Cu₂(SL)₂](PF₆)₂ (**2**), and [Cu₂(L)₂](PF₆)₂ (**3**) (LSH, R = –SCH₃; LH, R = H; Scheme 1). DFT calculations were also carried out, since this type

Scheme 1. Schematic Diagram of the Ligands HL and HSL



of calculation helps to understand the observed bulk magnetic properties.¹⁴

Experimental Section

All reagents were reagent grade and used without further purification unless stated otherwise. Solvents were of HPLC quality and were freshly distilled under nitrogen before use. Acetonitrile (CH₃CN) was distilled from calcium hydride.

Elemental analyses for C, H, and N were performed at the CEPEDQ (University of Chile) on a Fison-Carlo Erba EA 1108 model analyzer. Copper was determined by atomic absorption spectroscopy. IR spectra were obtained neat or as KBr pellets on a Bruker Vector 22 instrument. ¹H NMR spectra were recorded in CDCl₃ on a Bruker AMX-300 NMR spectrometer. Chemical shifts are reported as δ values downfield an internal Me₄Si reference.

Syntheses. 2-(Methylthio)-*p*-cresol was prepared from *p*-cresol according to the literature.¹⁵ 2-[(Bis(2-pyridylmethyl)amino)methyl]-4-methylphenol (HL) and 2-[(bis(2-pyridylmethyl)amino)methyl]-4-methyl-6-(methylthio)phenol (HSL) were synthesized by a Mannich reaction with bis(2-pyridylmethyl)amine,¹⁶ paraformaldehyde, and *p*-cresol or 2-(methylthio)-*p*-cresol, in 50 and 57% yield, respectively, as described for similar ligands.¹⁷

¹H NMR (CDCl₃) for HL: δ 10.8 (1H, broad, OH), 8.54 (2H, d, pyridine α protons), 7.58 (2H, t), 7.31 (2H, d) and 7.12 (2H, t) (pyridine protons), 6.95 (1H, d), 6.85 (1H, s), 6.80 (1H, d) (phenyl protons), 3.85 (4H, s, CH₂Py), 3.73 (2H, s, CH₂Ph), 2.21 (3H, s, CH₃Ph). ¹H NMR (CDCl₃) for HSL: δ 11.4 (1H, broad, OH), 8.58 (2H, d, pyridine α protons), 7.63 (2H, t), 7.36 (2H, d) and 7.16 (2H, t) (pyridine protons), 6.92 (1H, s), and 6.72 (1H, s) (phenyl protons), 3.86 (4H, s, CH₂Py), 3.75 (2H, s, CH₂Ph), 2.46 (3H, s, CH₃S), 2.26 (3H, s, CH₃Ph).

Syntheses of the Complexes. {[CuSL(Cl)]₂Cu}(PF₆)₂·H₂O (**1**). To a solution of the ligand HSL (2 mmol) and triethylamine (2 mmol) in methanol (10 mL) was added CuCl₂ (0.27 g, 3 mmol), and the mixture was refluxed for 60 min. Excess tetrabutylammonium hexafluorophosphate was added to the solution, and the crystalline product precipitated immediately. Recrystallization from boiling methanol affords crystals suitable for X-ray structural studies.

Anal. Calcd for C₄₂H₄₆Cl₂Cu₃F₁₂N₆O₃P₂S₂: C, 38.82; H, 3.57; N, 6.47; Cu, 14.67. Found: C, 39.12; H, 3.43; N, 6.64; Cu, 14.75.

[Cu₂(SL)₂](PF₆)₂ (**2**). This compound was obtained using the same procedure described for **1** but using equimolar quantities of CuCl₂ and the ligand. Single crystals suitable for X-ray structure determination were obtained by recrystallization from an acetonitrile–methanol solvent mixture.

- (1) Roth, A.; Becher, J.; Herrmann, C.; Görls, H.; Vaughan, G.; Reiher, M.; Klemm, D.; Plass, W. *Inorg. Chem.* **2006**, *45*, 10066–10076.
- (2) Crawford, V. H.; Richardson, H. W.; Wasson, J. R.; Hodgson, D. J.; Hatfield, W. E. *Inorg. Chem.* **1976**, *15*, 2107–2110.
- (3) Merz, L.; Haase, W. *J. Chem. Soc., Dalton Trans.* **1980**, 875–879.
- (4) Handa, M.; Koga, N.; Kida, S. *Bull. Chem. Soc. Jpn.* **1988**, *61*, 3853–3857.
- (5) Thompson, L. K.; Mandal, S. K.; Tandon, S. S.; Bridson, J. N.; Park, M. K. *Inorg. Chem.* **1996**, *35*, 3117–3125.
- (6) Xie, Y.-S.; Liu, X.-T.; Ni, J.; Liu, Q.-L. *J. Mol. Struct.* **2003**, *655*, 279–284.
- (7) Torelli, S.; Belle, C.; Gautier-Luneau, I.; Pierre, J. L.; Saint-Aman, E.; Latour, J. M.; Le Pape, L.; Luneau, L. *Inorg. Chem.* **2000**, *39*, 3526–2536.
- (8) Holz, R.; Brink, J. M.; Gobena, F. T.; O'Connor, J. *Inorg. Chem.* **1994**, *33*, 6086–6092.
- (9) Oberhausen, K. J.; Richardson, J. F.; Buchanan, R. M.; McCusker, J. K.; Hendrickson, D. N.; Latour, J.-M. *Inorg. Chem.* **1991**, *30*, 1357–1365.
- (10) Guerriero, P.; Tamburini, S.; Vigato, P. A. *Coord. Chem. Rev.* **1995**, *139*, 17–243.
- (11) Vigato, P. A.; Tamburini, S.; Fenton, D. E. *Coord. Chem. Rev.* **1990**, *106*, 25–170.
- (12) Borzel, H.; Comba, P.; Pritzkow, H. *Chem. Commun.* **2001**, 97–98.
- (13) *Magneto-Structural Correlations in Exchanged Coupled Systems*; Willett, D. D., Gatteschi, D., Kahn, O., Eds.; NATO-ASI Series; Reidel: Amsterdam, 1985.

- (14) Cauchy, T.; Ruiz, E.; Alvarez, S. *J. Am. Chem. Soc.* **2006**, *128*, 15722–15727.
- (15) Farrah, B. S.; Gilbert, E. E. *J. Org. Chem.* **1963**, *28*, 2807–2809.
- (16) Rojas, D.; García, A. M.; Vega, A.; Moreno, Y.; Venegas-Yazigi, D.; Garland, M. T.; Manzur, J. *Inorg. Chem.* **2004**, *43*, 6324–6330.
- (17) Itoh, S.; Takayama, S.; Arakawa, R.; Furuta, A.; Komatsu, M.; Ishida, A.; Takamuku, S.; Fukuzumi, S. *Inorg. Chem.* **1997**, *36*, 1407–1416.

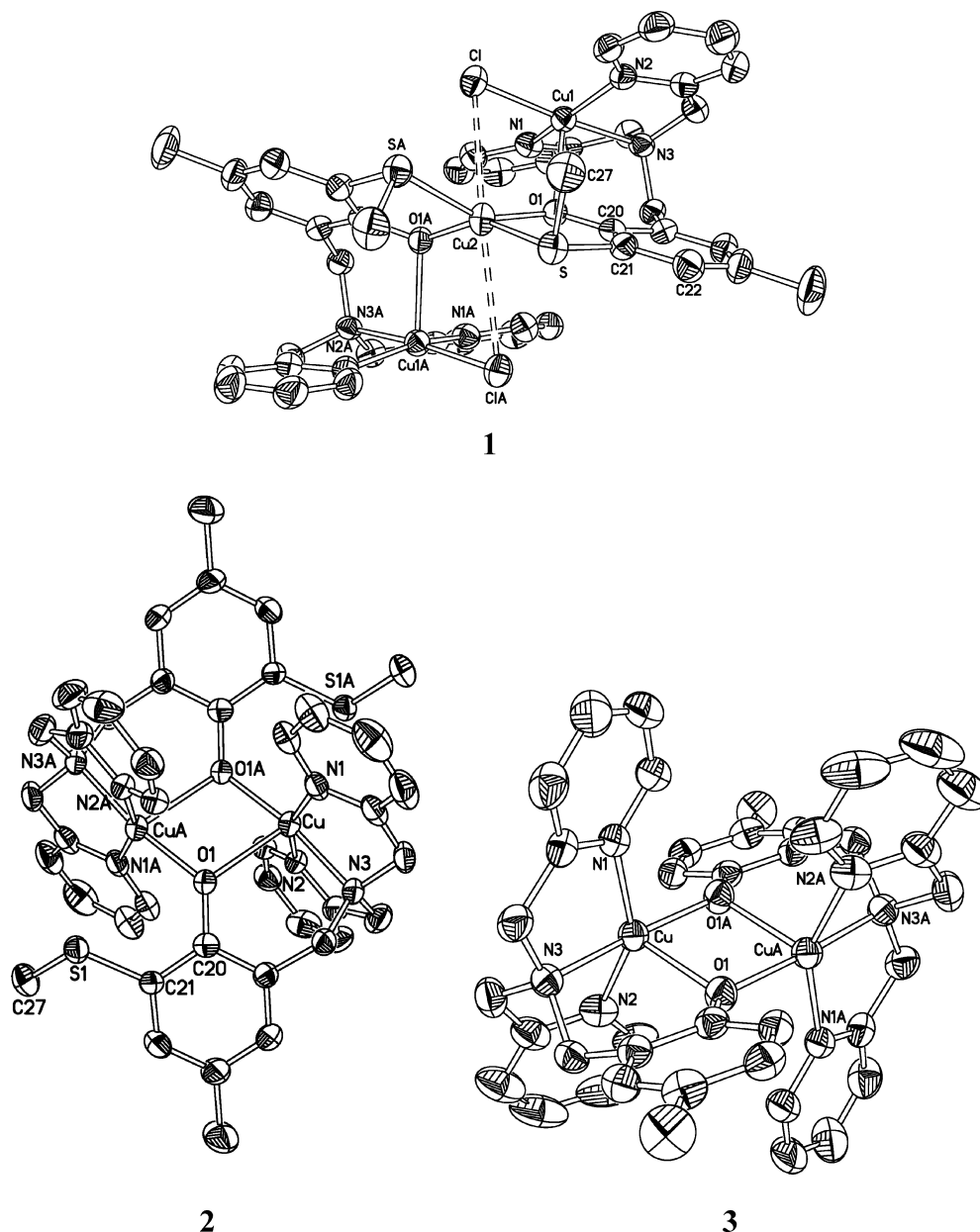


Figure 1. Molecular structure diagram for 1–3 with partial numbering scheme. Displacement ellipsoids are at the 33% probability level. The hexafluorophosphate counteranion, solvent molecules, and hydrogen atoms were omitted for clarity.

Anal. Calcd for $C_{42}H_{44}Cu_2F_{12}N_6O_2P_2S_2$: C, 44.00; H, 3.87; N, 7.33; Cu, 11.09. Found: C, 43.31; H, 3.81; N, 7.64; Cu, 11.35.

[Cu₂L₂](PF₆)₂ (3). To a solution of the ligand HL (2 mmol) and triethylamine (2 mmol) in methanol (10 mL) was added CuCl₂ (0.27 g, 2 mmol), and the mixture was refluxed for 60 min. Excess tetrabutylammonium hexafluorophosphate was added to the solution, and the crystalline product precipitated immediately. Recrystallization from acetonitrile–methanol afforded crystals suitable for X-ray structural studies.

Anal. Calcd for $C_{40}H_{40}Cu_2F_{12}N_6O_2P_2$: C, 45.57; H, 3.83; N, 7.97; Cu, 12.06. Found: C, 43.82; H, 3.74; N, 7.64; Cu, 12.56.

X-ray Crystallographic Data Collection and Refinement Details. For each compound a single crystal was mounted on the tip of a glass fiber. Diffracted intensities were collected on a Bruker Smart Apex diffractometer, using separations of 0.3° between frames and 10 s by frame. Data integration and absorption corrections were made using SAINT.¹⁸ The structures were solved using XS in SHELXTL^{18,19} by means of direct methods and completed

(non-H atoms) by Fourier difference synthesis. During the last stages of refinement some disorder on the hexafluorophosphate fluorine atoms of 2 was evident. It was modeled using two positions (A and B) for the six fluorine atoms, with partial occupancies of 0.57 and 0.43, respectively. These occupancies were then held constant during the last stages of refinement. Refinement until convergence was obtained using XL SHELXTL¹⁸ and SHELXL97.¹⁹ Figure 1 shows the molecular structure diagrams for 1–3. Additional crystallographic and refinement details are given in Table 1, and selected bond distances and angles are given in Table 2.

ESR and Magnetic Measurements. Magnetic susceptibility measurements for 1–3 were carried out on polycrystalline samples, at the Servei de Magnetoquímica of the Universitat de Barcelona, with a Quantum Design SQUID MPMS-XL susceptometer apparatus working in the range 2–300 K under magnetic fields of

(18) SHELXTL, version 5.1; Bruker AXS: Madison, WI, 1998.

(19) Sheldrick, G. M. SHELXL-97, Program for Crystal Structure Refinement; University of Göttingen: Göttingen, Germany, 1997.

Table 1. Crystallographic and Refinement Details for **1–3**

param	1	2	3
formula	C ₄₂ H ₄₆ Cl ₂ Cu ₃ F ₁₂ N ₆ O ₃ P ₂ S ₂	C ₄₂ H ₄₄ Cu ₂ F ₁₂ N ₆ O ₂ P ₂ S ₂	C ₄₀ H ₄₀ Cu ₂ F ₁₂ N ₆ O ₂ P ₂
Fw	1298.46	1145.99	1053.81
cryst syst	monoclinic	monoclinic	monoclinic
space group	<i>P2/c</i>	<i>C2/c</i>	<i>P2₁/n</i>
<i>a</i> /Å	15.742(2)	15.079(2)	11.242(1)
<i>b</i> /Å	12.085(1)	24.078(3)	16.762(2)
<i>c</i> /Å	15.706(2)	14.870(2)	11.965(1)
α /deg	90	90	90
β /deg	116.208(2)	116.272(2)	107.422(2)
γ /deg	90	90	90
<i>V</i> /Å ³	2680.9(5)	4841(1)	2151.3(4)
<i>Z</i>	1	4	2
<i>F</i> ₀₀₀	1310	2328	1068
<i>D</i> _c /g cm ⁻³	1.608	1.572	1.627
cryst size/mm ³	0.30 × 0.15 × 0.14	0.35 × 0.29 × 0.22	0.40 × 0.20 × 0.16
2 θ range/deg	3.38–50.32	3.46–50.14	4.32–50.16
μ /mm ⁻¹	1.501	1.120	1.159
index ranges	–18 ≤ <i>h</i> ≤ 18 –14 ≤ <i>k</i> ≤ 14 –18 ≤ <i>l</i> ≤ 18	–17 ≤ <i>h</i> ≤ 17 –28 ≤ <i>k</i> ≤ 28 –17 ≤ <i>l</i> ≤ 17	–13 ≤ <i>h</i> ≤ 13 –19 ≤ <i>k</i> ≤ 19 –14 ≤ <i>l</i> ≤ 14
no. of reflns colld	4802	4284	3815
no. of reflns obsd	2956	2497	2917
<i>R</i> , <i>R</i> _w ^a	0.0617, 0.1655	0.0689, 0.1946	0.0467, 0.1200
final diff/e Å ⁻³	0.581, –0.335	0.934, –0.559	0.592, –0.251

^a $R = \sum ||F_o| - |F_c|| / \sum |F_o|$. $R_w = [\sum w(|F_o| - |F_c|)^2 / \sum w(F_o)^2]^{1/2}$, where $w = 1/\sigma^2(F_o)$. $\lambda(\text{Mo K}\alpha) = 0.71073$.

Table 2. Selected Bond Distances and Angles for **1–3**^a

1		2		3	
Cu1–O1	2.256(4)	Cu–O1	2.406(4)	Cu–O1	2.182(2)
Cu2–O1	1.913(4)	Cu–N1	2.020(5)	Cu–N1	1.998(3)
Cu1–N1	1.989(5)	Cu–N2	2.002(5)	Cu–N2	2.015(3)
Cu1–N2	1.983(5)	Cu–N3	2.023(5)	Cu–N3	2.020(3)
Cu1–N3	2.052(4)	Cu–O1a	1.934(4)	Cu–O1a	1.924(2)
Cu1–Cl	2.252(2)	Cu–Cua	3.2794(14)	Cu–Cua	3.1147(8)
Cu2–Cl	3.173(2)	Cu–S1	2.9261(18)		
Cu2–Sa	2.294(2)				
Cu1–Cu2	3.4867(9)				
Cu1–Cu1a	5.7722(15)				
N1–Cu1–N2	159.0(2)	N2–Cu–N1	159.7(2)	N1–Cu–N2	150.3(1)
N1–Cu1–N3	81.8(2)	N1–Cu–N3	82.3(2)	N1–Cu–N3	83.6(1)
N2–Cu1–N3	83.3(2)	N2–Cu–N3	83.4(2)	N2–Cu–N3	82.2(1)
N1–Cu1–O1	98.1(2)	N1–Cu–O1	89.7(2)	N1–Cu–O1	101.3(1)
N2–Cu1–O1	97.2(2)	N2–Cu–O1	104.8(2)	N2–Cu–O1	105.0(1)
N3–Cu1–O1	92.5(2)	N3–Cu–O1	90.8(2)	N3–Cu–O1	91.9(1)
N1–Cu1–Cl	96.6(2)	O1–Cu–N1a	103.4(2)	O1–Cu–N1a	94.7(1)
N2–Cu1–Cl	96.8(2)	O1–Cu–N2a	92.6(2)	O1–Cu–N2a	102.4(1)
N3–Cu1–Cl	174.4(1)	O1–Cu–N3a	171.1(2)	O1–Cu–N3a	172.7(1)
O1–Cu1–Cl	93.1(1)	O1–Cu–O1a	82.5(2)	O1–Cu–O1a	81.5(1)
O1–Cu2–S	88.6(1)	Cu–O1–Cua	97.5(2)	Cu–O1–Cua	98.5(1)
O1–Cu2–Cl	75.6(1)				
O1–Cu2–Cla	84.7(1)				
S–Cu2–Cl	123.70(5)				
S–Cu2–Cla	78.23(5)				
S–Cu2–Sa	97.0(1)				
O1–Cu2–Sa	151.6(1)				
Cu1–O1–Cu2	113.3(2)				
Cu1–Cl–Cu2	77.96(5)				
Cu1–Cu2–Cu1a	111.74(4)				

^a Equivalent positions: **1**, (a) $-x + 2, -y, -z + 1$; **2**, (a) $-x + 1, y, -z + 1/2$; **3**, (a) $-x + 1/2, -y + 3/2, -z + 2$.

approximately 500 G (2–30 K) and 1000 G (35–300 K). Diamagnetic corrections were estimated from the Pascal tables. The ESR spectra have been recorded on an X-band Bruker spectrometer (ESR 300E).

Computational Details. Electronic structure calculations have been performed under a density functional theory approximation. The single point calculations were obtained with the Gaussian03 code²⁰ using the hybrid B3LYP functional.²¹ We have employed a triple- ζ all-electron Gaussian basis set proposed by Schaefer et al.

for all atoms.²² A guess function was generated with the JAGUAR 5.5 code.²³ The three calculations needed to obtain *J* (first neighbor interaction) and *J'* (second neighbor interaction) values correspond

(20) Frisch; et al. *Gaussian 03*, revision B.4; Gaussian, Inc.: Pittsburgh, PA, 2003.

(21) Becke, D. *J. Chem. Phys.* **1993**, *98*, 5648–5652.

(22) Schaefer, C.; Huber, R.; Ahlrichs, R. *J. Chem. Phys.* **1994**, *100*, 5829–5835.

(23) *Jaguar 5.5*; Schrödinger, Inc.: Portland, OR, 2003.

to an $S = 3/2$ solution and two $S = 1/2$ solutions. The methodology was previously reported by Ruiz et al.^{24–26} The spin density plot was performed with the Molekel code.²⁷

Results and Discussion

The preparation of **2** and **3** was straightforward, by treatment of a solution of copper dichloride with the ligand in refluxing methanol, in a one to one molar ratio. After addition of tetrabutylammonium hexafluorophosphate, the product crystallizes almost immediately. In a synthesis done with excess of copper chloride with the ligand HSL, we obtained two products, one of them corresponding to the trinuclear copper complex **1**. Almost quantitative production of this compound was obtained using a one to three ligand to copper molar ratio.

Description of Crystal Structures. $\{[\text{CuSL}(\text{Cl})_2\text{Cu}](\text{PF}_6)_2 \cdot \text{H}_2\text{O}\}$ (**1**). Compound **1** is a trinuclear copper complex which shows two different coordination environments, two square base pyramidal centers (Cu1, Cu1a, related by a C_2 axis) and a distorted square planar one (Cu2) (Figure 1). For each one of the pentacoordinated cupric centers, a deprotonated molecule of the ligand is tetracoordinated in a N,N',N'',O fashion, occupying three of the four basal positions with its nitrogen atoms, while the fourth is completed by a chloride anion. The phenoxo oxygen atom of the ligand lies in the apical position. Two of these monometallic units are coordinated to the central cupric ion by means of the sulfur from the SCH_3 substituent and a bridging phenoxo oxygen atom, thus defining a cis configuration for the ligands around the central copper atom, Cu2. The Cu2–S distance is 2.294 Å, as expected for a coordinated thioether group. Selected bond distances and angles are given in Table 2.

The coordination geometry around Cu1 is slightly distorted, with $\tau^{28} = 0.26$, while the environment around Cu2 is noticeably distorted from a square plane, with a dihedral angle between the O1–Cu2–S and O1a–Cu2–Sa planes of 41.1° , instead of the expected 0° . This can be ascribed to steric hindrance of the methyl groups in the cis-configuration observed for the SCH_3 substituent. The long distance measured between the chloride anion (Cl) and Cu2, 3.173 Å, precludes considering the coordination geometry as octahedral.

The phenoxo oxygen atom that bridges the two cupric centers is axial for Cu1 but equatorial for Cu2, and therefore, the bridging mode is axial–equatorial. This leads to a Cu_2O (Cu1–O–Cu2) asymmetric triangle, with one of the sides being 1.913(4) Å (Cu1–O1) while another one is 2.256(4) Å (Cu2–O1). These values are in the range observed in reported copper complexes with phenoxo ligands.^{17,29,30} The bridging Cu1–O–Cu2 angle is $113.27(17)^\circ$, and the phenyl

group of the Ph–O is out of the Cu_2O plane by 45.6° . This last value is the angle between the Cu_2O plane and the O1–C20 vector. The phenyl ring is also twisted around the C–O axis with respect to the Cu_2O plane, the dihedral angle between the phenoxo moiety and the Cu_2O plane being 55.0° . The thiomethyl group lies out of the plane of the phenyl ring, the C22–C21–S–C27 torsion angle being $74.0(5)^\circ$.

The three copper(II) centers of the molecule define an isosceles triangle, with two sides equal to the intramolecular nearest-neighbor distance (Cu1–Cu2), 3.487 Å. The third triangle side corresponds to the distance between the “terminal” centers (Cu1–Cu1a), 5.7722(15) Å. The Cu1–Cu2–Cu1a angle is $111.74(4)^\circ$.

$[\text{CuSL}]_2(\text{PF}_6)_2$ (**2**). Figure 1 shows the molecular structure diagram of **2**, and selected bond distances and angles are given in Table 2. The cation of **2** is a centrosymmetric dinuclear complex formed by two distorted square base pyramidal copper(II) centers ($\tau = 0.22$). Each copper(II) ion is coordinated to the tertiary amine and two pyridine nitrogens of the SL ligand anion in the basal plane, while the axial position is occupied by the phenoxo group. A phenoxo group from the ligand of the second copper ion occupies the fourth basal position to form an unsymmetrically bridged Cu_2O_2 core. The two parts of the dimer are trans to each other, and the Cu–Cu distance is 3.2794(14) Å. The Cu_2O_2 core is strictly planar, because of the inversion center in the middle point of Cu–Cu, with a Cu–O–Cu angle of $97.5(2)^\circ$. The parallelogram is asymmetric, with the Cu–O_{eq} distance of 1.934(4) Å and the Cu–O_{ax} distance of 2.406(4) Å.

The phenyl group for **2** is also out of the Cu_2O plane, as observed in **1**. The dihedral angle between the Cu_2O plane and the O1–C20 vector is 49.8° . The twisting of the phenyl ring around C–O with respect to the Cu_2O plane is 45° for this compound.

The Cu–S bond distance is relatively long (2.9261(4) Å), consistent with a weak thioether interaction, as observed for a similar copper complex (Cu–S = 2.765 Å).³¹ An electronic perturbation of the thioether group due to this interaction is reflected in the bond angles around S, which show a deviation toward pyramidal geometry, resulting in a torsion angle (C22–C21–S–C27) of $41.4(5)^\circ$ compared with the same angle in **1** of $74.0(6)^\circ$. Similar geometric distortions have been reported^{31–33} for copper complexes with other thioether-donating ligands where the effects of S bonding on the valence electronic structure are reflected in the geometry around the sulfur atom; the shorter the Cu–S distance and, hence, a stronger interaction are reflected in a more pronounced deviation from planarity as seen in **1** (Cu2–S distance = 2.294 Å; torsion angle (C22–C21–S–C27) of $74.0(5)^\circ$). The thiomethyl S-atom does not coordinate

(24) Ruiz, E.; Cano, J.; Alvarez, S.; Alemany, P. *J. Comput. Chem.* **1999**, *20*, 1391–1400.

(25) Ruiz, E.; Rodriguez-Fortea, A.; Cano, J.; Alvarez, S.; Alemany, P. *J. Comput. Chem.* **2003**, *24*, 982–989.

(26) Ruiz, E. *Struct. Bonding* **2004**, *113*, 71–102.

(27) Portmann, S. *Molekel 4.3*; Université de Genève: Genève, Switzerland, 1992.

(28) Addison, A. W.; Rao, T. N.; Reedijk, J.; Van Rijn, J.; Verschoor, G. C. *J. Chem. Soc., Dalton Trans.* **1984**, 1349–1356.

(29) Shimazaki, Y.; Huth, S.; Hirota, S.; Yamauchi, O. *Inorg. Chim. Acta* **2002**, *331*, 168–170.

(30) Murray, S. G.; Hartley, F. R. *Chem. Rev.* **1981**, *81*, 365–414.

(31) Taki, M.; Hattori, H.; Osako, T.; Nagatomo, S.; Shiro, M.; Kitagawa, T.; Itoh, S. *Inorg. Chim. Acta* **2004**, *357*, 3369–3381.

(32) Blake, A. J.; Schröder, M. *Adv. Inorg. Chem.* **1990**, *35*, 1–80.

(33) Whittaker, M. M.; Chuang, Y.-Y.; Whittaker, J. W. *J. Am. Chem. Soc.* **1993**, *115*, 10029–10035.

to the Cu(II) ion [$\text{Cu}-\text{S} = 4.606(2) \text{ \AA}$] in the complex $\text{LMeSMeCu}(\text{O}_2\text{CCH}_3)$ ($\text{LMeSMe} = 1$ -(2-hydroxy-5-methyl-3-(methylthio)benzyl)-4,7-diisopropyl-1,4,7-triazacyclononane) reported by Tolman et al.,³⁴ leading to a coplanar thiomethyl group with the phenolate ring (the torsion angle is only $-0.3(6)^\circ$).

[CuL]₂(PF₆)₂ (3). Compound **3** is a dimer with two equivalent Cu centers related by an inversion center located in the middle of the two copper atoms. Figure 1 shows the molecular structure diagram of **3**, and Table 2 gives selected bond distances and angles. The coordination geometry around each metal center is a distorted square base pyramidal ($\tau = 0.37$). The coordination sphere around each copper center is formed by the amine nitrogen and the two pyridine nitrogens in the basal plane, while the axial position is occupied by the phenoxo group. The fourth equatorial position is occupied by a phenoxo group of the neighboring molecule similar to the structure of **2**. The central Cu_2O_2 core is also planar, because of the inversion center with a Cu–Cu distance of 3.115 Å and an Cu–O–Cu angle of $98.5(1)^\circ$ which is close to the one measured for **2**, $97.5(2)^\circ$. The Cu_2O_2 core is asymmetric, with Cu–O_{eq} and Cu–O_{ax} of 1.924(4) and 2.182(4) Å, respectively. The angle defined by the C–O(phenoxo) vector and the Cu_2O_2 plane is 55° , and the phenyl ring is similarly twisted with respect to the Cu_2O plane by 27° .

All three complexes exhibit axial–equatorial phenoxo bridging between the metal centers. It has been suggested that the nature of chelate rings formed and the resultant steric factors involved are responsible for the coordination mode of the phenolate ion; thus, copper complex of a tripodal ligand, having a phenolate moiety with 6,6,6-membered chelate ring sequence, tends to take the phenolate moiety as an equatorial ligand.³⁵ The present complexes possess a 5,5,6-chelate ring sequence, and the phenoxo ion coordinates in the axial position as in other complexes with this same ring sequence.³⁶ Equatorial coordination of the phenoxo group has been reported in complexes having similar ligands with 5,5,6 ring sequence but with methyl substituent in the ortho position to the nitrogen donor.^{29,31} As a result of the steric effect of the methyl substituent, the nitrogen donor occupies the axial position, while the phenoxo becomes equatorially coordinated. Since in the present complexes there are no such steric effects, the phenoxo coordinates to the more accessible axial position. The vacant equatorial position is then occupied by a phenolate group of a neighboring molecule resulting in an axial–equatorial bridging mode of the two copper centers in the dinuclear moiety.

ESR and Magnetic Properties. Magnetic Behavior of

1. The shape of the $\chi_{\text{M}}T$ vs T curve indicates a dominant ferromagnetic coupling, which results from the interaction

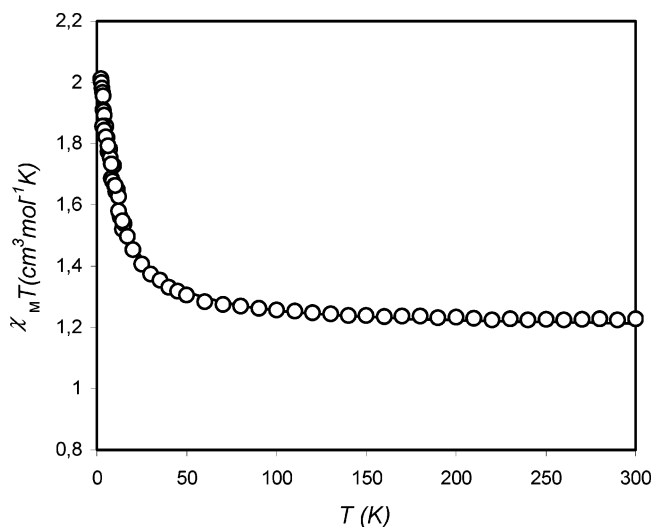


Figure 2. Plot of the $\chi_{\text{M}}T$ product vs T for **1** (per Cu_3). The solid line shows the best fit of the data (see text).

between the copper(II) atoms (Figure 2). At room temperature the $\chi_{\text{M}}T$ value is $1.228 \text{ cm}^3 \text{ K mol}^{-1}$, which is close to the expected value for three uncoupled copper(II) ions. $\chi_{\text{M}}T$ increases slightly with lowering of temperature and reaches a value of $2.011 \text{ cm}^3 \text{ mol}^{-1} \text{ K}$ at ca. 2 K.

The exchange parameters between the copper(II) atoms were determined by fitting the $\chi_{\text{M}}T$ data by means of least squares to the expression (1),³⁷ where N is Avogadro's number, μ_{B} is the Bohr magneton, and k is the Boltzmann constant. In a first approximation, considering $J' = 0$ and $g_{\text{A}} = g_{\text{B}}$, the best fit of the experimental data was obtained with $J = +5.7 \text{ cm}^{-1}$ and $g = 2.07$ with $R = 2.4 \times 10^{-5}$ ($R = \sum_i (\chi_{\text{M}}T_{\text{icalc}} - \chi_{\text{M}}T_{\text{ixp}})^2 / (\chi_{\text{M}}T_{\text{ixp}})^2$):

$$\chi_{\text{M}} = \frac{N\mu_{\text{B}}^2}{4kT} \frac{g_{1/2,1}^2 + g_{1/2,0}^2 \exp((J - J')/kT) + 10g_{3/2,1}^2 \exp(3J/2kT)}{1 + \exp((J - J')/kT) + 2 \exp(3J/2kT)} \quad (1)$$

Here, $g_{1/2,1} = (4g_{\text{A}} - g_{\text{B}})/3$, $g_{3/2,1} = (2g_{\text{A}} + g_{\text{B}})/3$, and $g_{1/2,0} = g_{\text{B}}$.

The field dependence of magnetization (0–5 T) measured at 2 K is shown in Figure S1, in the form of $M/N\beta$ (per Cu_3 unit) vs H . The magnetization reaches a value of $2.95 N\beta$ at 5 T, which is close to the expected $S = 3/2$ value of 3 Cu atoms coupled ferromagnetically.

The ESR spectrum of **1** recorded in X band at room temperature (Figure S2) shows an isotropic signal which corresponds to the transition $\Delta M_{\text{S}} = \pm 1$, centered at $g = 2.1$ (3330 G for $\nu = 9.7934 \text{ GHz}$), with a peak-to-peak line width ΔB_{pp} of 30 G.

DFT calculations for complex **1** were done considering a general spin Hamiltonian (eq 2). The general spin Hamiltonian includes one first-neighbor coupling constant (J), as well as the exchange coupling term between second neighbors (J'), where \hat{S}_i are the spin operators of each paramagnetic copper(II) center:

(37) Kahn, O. *Molecular Magnetism*; VCH Verlagsgesellschaft: Weinheim, Germany, 1993.

(34) Halfen, J. A.; Jazdzewski, B. A.; Mahapatra, S.; Berreau, L. M.; Wilkinson, E. C.; Que, L., Jr.; Tolman, W. B. *J. Am. Chem. Soc.* **1997**, *119*, 8217–8227.

(35) Adams, H.; Bailey, N. A.; Campbell, I. K.; Fenton, D. E.; He, Q.-Y. *J. Chem. Soc., Dalton Trans.* **1996**, 2233–2237.

(36) Vaidyanathan, M.; Viswanathan, R.; Palaniandavar, M.; Balasubramanian, T.; Prabhakaran, P.; Muthiah, T. P. *Inorg. Chem.* **1998**, *37*, 6418–6427.

$$\hat{H} = -J[\hat{S}_1\hat{S}_2 + \hat{S}_2\hat{S}_3] - J'[\hat{S}_1\hat{S}_3] \quad (2)$$

In order to calculate the exchange coupling constants, the whole X-ray structure of the complex including the three copper(II) centers was employed. The obtained exchange coupling constants are $J = +11.7 \text{ cm}^{-1}$ and $J' = -0.05 \text{ cm}^{-1}$. The analysis of the results reveals that a ferromagnetic coupling occurs between first neighbors and a weak anti-ferromagnetic interaction between second-neighbors.

Using the topological model for trinuclear species (eq 1) with $J = +11.7$ and $J' = -0.05 \text{ cm}^{-1}$ and $g_A = 2.07$ and $g_B = 2.03$, a good simulation of the experimental data was obtained (Figure 2).

The use of the simplified model to fit the experimental magnetic data of **1**, which takes into account only a first neighbor interaction ($J' = 0$), gives a ferromagnetic phenomenon with a J value of $+5.7 \text{ cm}^{-1}$. DFT calculations permit one to confirm the ferromagnetic interaction between first neighbors but with a higher value for J ($J = +11.7$). In addition, a very weak antiferromagnetic exchange for **1** was obtained for the second-neighbor interaction, with a J value of -0.05 cm^{-1} .

An analysis of the calculated spin densities of **1** shows a delocalization mechanism. Even though the Heisenberg model assumes localized spins on the metal atoms, the delocalization mechanism reveals partially localized spin densities on the copper atoms and spin densities on the atoms of the first coordination sphere. The shape of the spin density at each copper center corresponds to a $t_{2g}^6e_g^3$ electronic configuration. The spin density distribution is similar to the shape of the superimposed three SOMO's of the molecule (Figure 3).³⁸

Taking into account that the amount of spin delocalization toward the ligand atoms represents a covalent character of the metal ligand bond, it is also possible to infer a high degree of interaction between the copper atom and the sulfur atom of the ligand, as found by X-ray diffraction.

Magnetic Behavior of 2 and 3. The magnetic behavior of **2** and **3** is shown in Figures 4 and 5, as $\chi_M T$ vs T plots. At room temperature the $\chi_M T$ values are 0.863 and $0.831 \text{ cm}^3 \text{ K mol}^{-1}$ for **2** and **3**, respectively, which are close to the expected value for two uncoupled copper(II) ions ($0.74 \text{ cm}^3 \text{ K/mol}$ two copper(II) with $g = 2.0$). The $\chi_M T$ product behaves in a different way for **2** and **3**; for **2** it increases slightly with lowering of temperature and reaches a value of $1.020 \text{ cm}^3 \text{ mol}^{-1} \text{ K}$ at ca. 2 K. The shape of this curve indicates dominant ferromagnetic coupling, which results from the interaction between the copper(II) atoms. Instead, for **3** the overall magnetic behavior corresponds to an antiferromagnetically coupled system. When the sample is cooled, the $\chi_M T$ decreases slowly and below 100 K decreases more rapidly to $0.0013 \text{ cm}^3 \text{ mol}^{-1} \text{ K}$ at 2 K. The χ_M value increases continuously on cooling to reach a maximum of $0.027 \text{ cm}^3 \text{ mol}^{-1} \text{ K}$ at 17 K and decreases to zero at 2 K.

The experimental data were fitted to the Bleaney–Bowers expression for an isotropically coupled pair of $S = 1/2$ ions

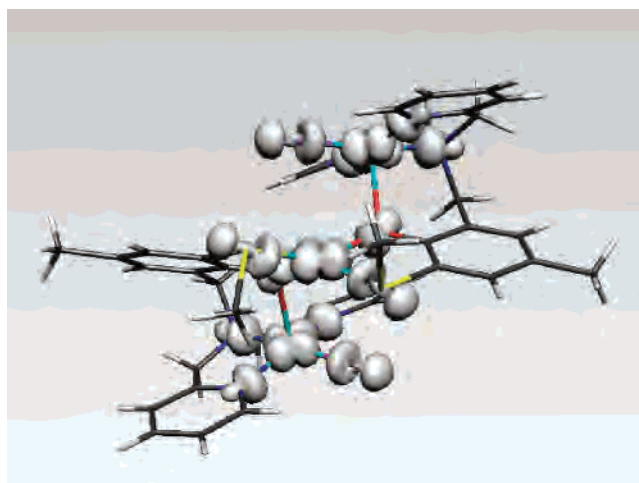


Figure 3. Spin density surface for **1** ($S = 3/2$). Gray color: α spin density.

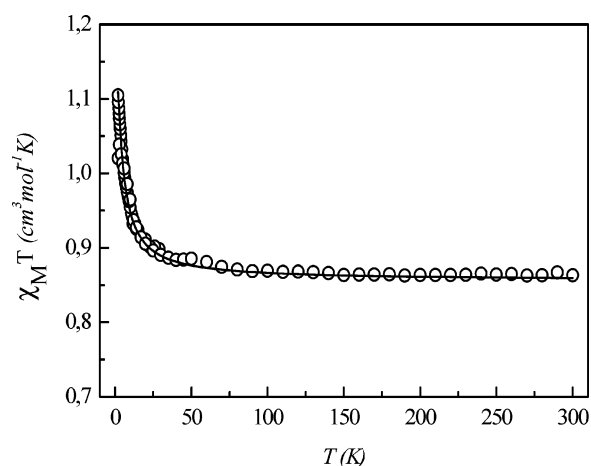


Figure 4. Plot of the $\chi_M T$ product vs T for **2** (per Cu₂). The solid line shows the best fit of the data (see text).

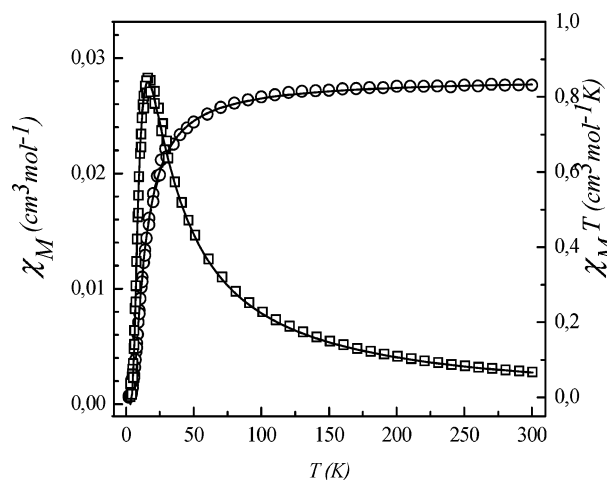


Figure 5. Plots of the χ_M (\square) and $\chi_M T$ product vs T (\circ) for **3** (per Cu₂). The solid line shows the best fit of the data (see text).

(eq 3),³⁹ where the symbols have their usual meaning. The best-fit parameters for reproducing satisfactorily the experimental data, as shown in Figures 4 and 5, are $J = +3.4 \text{ cm}^{-1}$ and $g = 2.14$ with $R = 3.7 \times 10^{-5}$ ($R = \sum_i (\chi T)_{\text{calc}} -$

(38) Ruiz, E.; Cirera, J.; Alvarez, S. *Coord. Chem. Rev.* **2005**, *249*, 2649–2660.

(39) Bleaney, B.; Bowers, K. D. *Proc. R. Soc. London, Ser. A* **1952**, *214*, 451–465.

$\chi T_{\text{exp}}/(\chi T_{\text{exp}})^2$ for **2** and $J = -16.7 \text{ cm}^{-1}$ and $g = 2.11$ with $R = 4.1 \times 10^{-5}$ ($R = \sum_i (\chi_{\text{calc}} - \chi_{\text{exp}})^2 / (\chi_{\text{exp}})^2$) for **3**:

$$\chi_M = \frac{Ng^2\mu_B^2}{kT} \frac{2 \exp(J/kT)}{1 + 3 \exp(J/kT)} \quad (3)$$

The field dependence of magnetization (0–5 T) measured at 2 K for **2** is shown in Figure S3, in the form of $M/N\beta$ (per Cu_2 unit) vs H . The magnetization reaches a value of $2.03 N\beta$ at 5 T, which is close to the expected $S = 1$ value of two copper(II) atoms coupled ferromagnetically.

The ESR spectra of **2** and **3** recorded in X band at room temperature are shown in Figure S4. Compound **2** shows two bands at $g_{\parallel} = 2.19$ and $g_{\perp} = 2.07$ (3192 and 3373 G for $\nu = 9.7941 \text{ GHz}$), corresponding to the transition $\Delta M_S = \pm 1$. The ESR spectra of **3**, at first sight, seem to correspond to a triplet state, with a central band located at 2145 G. The two bands located at side are observed at 2731 and 3900 G for $\nu = 9.77931 \text{ GHz}$, corresponding to the “z” component of the \mathbf{g} tensor separated into two bands due to the zero-field splitting (ZFS or D), which is of 0.06 cm^{-1} approximately. The same would happen with the “x” and “y” components, but the corresponding signals are not located inside the encircling of the central band. In addition, the spectrum shows a band at half-field at $g = 4.54$ (1526 G) corresponding to the transition $\Delta M_S = \pm 2$.

The magnitude of the magnetic exchange interactions between copper(II) ions in binuclear complexes is dependent upon the orbital ground-state configuration of the copper(II) ions. Strong magnetic exchange interactions require both good σ -bonding orientation of the magnetic orbitals (i.e., the orbitals that contain the unpaired electrons) and good superexchange pathways provided by the bridging atom orbitals.^{40–43}

The results of the reported structural studies for **2** and **3** show that the copper(II) ions have distorted square-pyramidal coordination geometries bridged by two phenoxo groups in an axial–equatorial fashion. The bridging phenoxo oxygen, being in the axial position relative to one copper(II) ion and equatorial to the other one, has bonding interactions with the d_{z^2} and $d_{x^2-y^2}$ orbitals of Cu_1 and Cu_2 , respectively. Thus, the oxygen atoms do not mediate a strong interaction between the two metal centers.⁴⁴ Accordingly, the magnetic susceptibility data obtained on **2** and **3** confirm weak magnetic exchange interactions, with $J = +3.4$ and -16.7 cm^{-1} , respectively.

Figure 6 shows the calculated spin density for the $S = 1$ state of **2**. The oxygen and nitrogen atoms from the first coordination sphere of both copper centers present α spin density as a consequence of a delocalization mechanism with

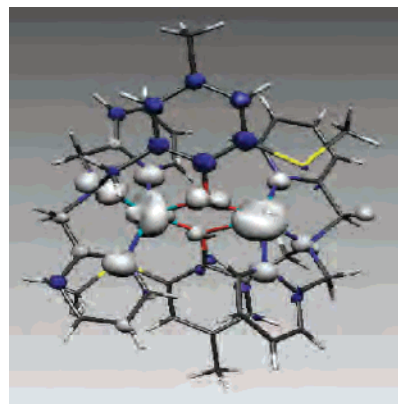


Figure 6. Spin density surface for **2** ($S = 1$): (gray) spin α ; (blue) spin β .

the metal centers. The spin density on the metal centers shows for one copper a surface largely related to a d_{z^2} orbital, while the other copper(II) center surface can be described as a mixture of $d_{x^2-y^2}$ and d_{xy} orbitals. This mixture of orbitals can be due to the large geometrical distortion observed for both metal centers. It is interesting to point out that β spin density is observed mainly allocated on one phenyl group and corresponds to a polarization mechanism. The low calculated spin density on the sulfur atoms, compared to that obtained for the other atoms of the first coordination sphere of the copper centers, suggests a weak interaction as was initially proposed from the crystallographic data for **2** (2.93 Å). The Cu–S distance in compound **1** is 2.29 Å, and in terms of spin density, it is clearly observed a high α spin density on the sulfur atoms due to a direct delocalization mechanism with the copper center and to a strong bonding interaction as was mentioned before.

The calculated spin density distribution for **3** is given in Figure S5. The nitrogen atoms of the first coordination sphere of each copper(II) center show spin density with a sign, which is related to the metal atom to which they are bonded. In the case of the phenoxo oxygen atoms, one has α spin and the other β spin, showing a symmetrical distribution. The shape of the spin density at each of the metal centers seems to correspond to a hybridization of d orbitals. The distorted square-base pyramid of each copper center(II) ($\tau = 0.373$) could explain the observed mixture of the involved orbitals.

As mentioned above, the equatorial–axial configuration of the phenoxo bridges in **1–3** precludes a strong magnetic exchange between the copper centers. To rationalize the observed differences in magnetic behavior, one may take into account the distortions in the coordination spheres of the reported complexes.

Two geometrical parameters have been used to explain the nature of the magnetic exchange constants in binuclear copper(II) complexes. In the case of the biphenoxo-bridged complexes, the difference in sign of the J values has been related to the magnitude of the bridging angle Cu–O–Cu° and the planarity of the phenyl ring in relation to the Cu_2O_2 plane. For **2**, the value of the angle is 97.5° , while for **3** this same angle is 98.5° . The compound with the slightly larger bridging angle presents weak antiferromagnetism. Also, the

(40) Felthouse, T. R.; Laskowski, E. J.; Hendrickson, D. N. *Inorg. Chem.* **1977**, *16*, 1077–1089.

(41) Hay, P. J.; Thibeault, J. C.; Hoffmann, R. *J. Am. Chem. Soc.* **1975**, *97*, 4884–4899.

(42) Doman, T. N.; Williams, D. E.; Banks, J. F.; Buchanan, R. M.; Chang, H.-R.; Webb, R. J.; Hendrickson, D. N. *Inorg. Chem.* **1990**, *29*, 1058–1062.

(43) Berends, H. P.; Stephan, D. W. *Inorg. Chem.* **1987**, *26*, 749–754.

(44) Cervera, B.; Ruiz, R.; Lloret, F.; Julve, M.; Cano, J.; Faus, J.; Bois, C.; Mrozinski, J. *J. Chem. Soc., Dalton Trans.* **1997**, 395–401.

phenyl group of the phenoxo moiety for **2** is out of the Cu_2O_2 plane, with the angle between the plane and the O1–C20 vector of 138.42° , while for **3** this same angle is 158.31° . Thus, the more planar system, corresponding to **3**, presents an antiferromagnetic exchange interaction.

The trinuclear complex **1** can be described, from a magnetic point of view, as constituted of two dinuclear units Cu1–Cu2 and Cu1a–Cu2 . For **1**, only one phenoxo bridge is observed for each dimeric unit, which can be considered as an exchange pathway for the magnetic coupling interaction. Even though the bridging Cu1–O–Cu2 angle is obtuse with a value of 113.27° , the magnetic exchange interaction is weakly ferromagnetic. Therefore, the observed ferromagnetism may be correlated to the out of plane position of the phenyl ring with respect to the Cu_2O_2 plane.

For comparison, the magnetic exchange coupling observed for other binuclear copper(II) complexes with one equatorial–axial phenoxo bridge, such as $[\text{Cu}_2(\text{BIMP})(\text{H}_2\text{O})_2]^{3+}$ and $[\text{Cu}_2(\text{BBMP})(\text{H}_2\text{O})_2]^{3+}$, is weakly ferromagnetic ($+0.27$ and $+4.2 \text{ cm}^{-1}$).^{9,43} Other examples are $[\text{Cu}_2(\text{BPMP})(\text{H}_2\text{O})_2]^{3+}$ and $[\text{Cu}_2(\text{CH}_3\text{HXTA})(\text{H}_2\text{O})_2]^-$, which are essentially uncoupled^{7,8} ($\text{H–BIMP} = 2,6\text{-bis}[(\text{bis}((1\text{-methylimidazol-2-yl})\text{-methyl})\text{amino})\text{methyl}]\text{-4-methylphenol}$; $\text{H–BBMP} = 2,6\text{-bis}[(\text{bis}(\text{benzimidazolymethyl})\text{amino})\text{methyl}]\text{-}p\text{-cresol}$; $\text{H–BPMP} = 2,6\text{-bis}[(\text{bis}(2\text{-pyridylmethyl})\text{amino})\text{methyl}]\text{-4-methylphenol}$; $\text{CH}_3\text{HXTA} = N,N'\text{-(2-hydroxy-5-methyl-1,3-xylylene)bis}(N\text{-carboxymethylglycine})$). However, a strong antiferromagnetic coupling is observed for the binuclear copper(II) complex $[\text{Cu}_2(\text{CH}_3\text{HXTA})\text{Py}_2]^-$, since in this complex the μ -phenoxo oxygen bond is equatorial to both Cu1 and Cu2 .⁴⁵

Conclusions

We have prepared and structurally and magnetically characterized a series of Cu(II) complexes with two new tripodal ligands, containing a phenoxo moiety with axial–

equatorial coordination of this group to the metal centers due to the 5,5,6 ring sequence. Compound **1** is monobridged, while **2** and **3** are bibriged. The three studied complexes present magnetic exchange pathways through axial–equatorial phenoxo groups, leading to weak magnetic interactions.

Compound 1. The exchange constant calculated using the B3LYP functional shows the presence of ferromagnetic interaction for first neighbor atoms. The calculated interaction between second neighbors is very weakly antiferromagnetic. The obtained J ($+11.7 \text{ cm}^{-1}$) and J' (-0.05 cm^{-1}) values reproduce the experimental data.

Using the simplified model ($J' = 0$ and $g_A = g_B$), the best fit of the experimental data was obtained with $J = +5.7 \text{ cm}^{-1}$, which also corresponds to a ferromagnetic behavior.

Compounds 2 and 3. The magnetic susceptibility data obtained on **2** and **3** show magnetic exchange interactions with $J = +3.4$ and -16.7 cm^{-1} , respectively. The difference in sign of the J values can be related to the magnitude of the bridging angle Cu–O–Cu and the planarity of the phenyl ring in relation of the Cu_2O_2 plane. Thus, the more planar system corresponding to **3** presents an antiferromagnetic exchange interaction.

Of the three studied complexes, two new examples of ferromagnetically coupled copper(II) complexes, **1** and **2**, are reported.

Acknowledgment. Financial support from Project FONDECYT 1050484 is gratefully acknowledged. Support from grants given by the Ministerio de Educación y Ciencia de España (Programa Ramón y Cajal) and BQU2003/00538 is also gratefully acknowledged. E.S. and D.V.-Y. acknowledge FONDAP 11980002 and Proyecto Bicentenario de Inserción Académica for financial support.

Supporting Information Available: Magnetization curves, ESR spectra, and spin density surfaces in Figures S1–S5 and crystallographic data in CIF format for complexes **1–3**. This material is available free of charge via the Internet at <http://pubs.acs.org>.

IC700544B

(45) Holz, R. C.; Bradshaw, J. M.; Bennett, B. *Inorg. Chem.* **1998**, *37*, 1219–1225.